Journal of Nano- and Electronic Physics
Vol. **18** No 3, 03007(5pp) (2026)

Журнал нано- та електронної фізики
Том **18** № 3, 03007(5cc) (2026)

OPEN ACCESS

REGULAR ARTICLE

Color-Tunable Quantum Well Based Organic Light-Emitting Device

Mykhailo Shchetinin* ✉, Stepan Kutsiy, Mykhailo Hladun, Iryna Yaremchuk, Pavlo Stakhira

Department of Electronic Devices, Lviv Polytechnic National University, 79013 Lviv, Ukraine

(Received 04 February 2026; revised manuscript received 20 June 2026; published online 26 June 2026)

The development of efficient organic light emitting devices (OLEDs), particularly those based on thermally activated delayed fluorescence (TADF), is quite often struggling from high non-radiative recombination rate and exciton quenching in case of the neat film, which is frequently usual for complex host-guest systems. This study proposes an alternative multiple quantum well architecture to achieve controlled color modulation and flexible emissive performance using a solvatochromic acceptor orange-red emitter, NI-3TPA. By utilizing mCBP as the wide-bandgap barrier layer, OLEDs featuring varying quantum well thickness (3nm to 7 nm) were fabricated and systematically evaluated against the non-doped device as well as referenced host-guest structure.

The results demonstrate that modifying the mCBP barrier thickness directly influences electroluminescent characteristics. Specifically, reducing the barrier to 3nm enhances the carrier tunneling probability, thereby effectively suppressing exciton quenching. The optimized 3nm quantum well based device demonstrated a reduced turn-on voltage of 5.6 V and achieved a maximum external quantum efficiency (EQE) of 2.03 % which outperforms the 7nm device (1.07 %) and the neat-film device (0.83 %). All fabricated devices exhibited strong light emitting within. red-to-orange CIE1931 color coordinates.

The proposed architecture demonstrates precise tuning of the electroluminescence spectrum, exhibiting a redshift from 566nm to 578 nm as the potential well width increased due to the quantum confinement effect. This paper concludes that the quantum well strategy provides a reproducible approach for localizing charge carriers and excitons within the emissive layer, mitigating parasitic processes and side effects such as intermolecular and exciton quenching without complex fabrication processes.

Keywords: OLED, TADF, Quantum Well, Red-Yellow Emitter, EQE.

DOI: 10.21272/jnep.18(3).03007 PACS number: 620.9

1. INTRODUCTION

The modern strategy for the design of red organic emitters involves constructing a twisted donor-acceptor (D-A) conjugated scaffold with appropriate intramolecular charge transfer (ICT) characteristics. Such an ambipolar system significantly impacts the frontier molecular orbital levels, generates long-wavelength emission, and facilitates the tuning of optical and electronic properties. Recent developments in the field of red OLEDs have primarily focused on donor-acceptor (D-A) materials, exhibiting thermally activated delayed fluorescence (TADF). These materials enable a theoretical internal quantum efficiency (IQE) of 100 % through reverse intersystem crossing (RISC) mechanism which transfers triplet states into singlet ones [1]. According to energy gap law [2], the significant non-radiative recombination rate (k_{nr}) of red TADF emitters often leads to relatively low external quantum efficiency (EQE) [3, 4]. It is evident that low emissive performance limits the commercial viability of red OLEDs for practical applications, despite the inherent advantages of organic light-emitting devices, such as mechanical flexibility, cost-effectiveness and potential biocompatibility. To mitigate exciton quenching effects within the OLED architecture, TADF emitters are utilized as guest dopants in a host-guest matrix [5, 6]. In a host-guest system, excitons are initially generated in the host component and subsequently transferred to the guest emitter. Consequently, achieving high-performance OLEDs requires efficient exciton transfer and effective confinement within the emissive layer (EML). Furthermore, the host component can modulate the emission spectrum of the guest emitter due to varying polarity, providing a mechanism for color tuning in OLED displays. However, this approach poses a complex technological challenge with frequently non-reproducible results, which limits the fabrication of red OLEDs.

An alternative approach to solve this issue is the utilization of a multiple quantum well structure, which serves as an effective method for enhancing the performance and characteristics of red OLEDs [7]. Such architecture does not require the need for a complex OLED fabrication process. With this strategy, the localization of both charge carriers and excitons occurs within the limits of the EML. Consequently, the radiative recombination efficiency of the carriers can be significantly improved.

These considerations defined the objective of the present study, which aimed at the controlled modulation of the electroluminescence (EL) spectral range for an or-

* Correspondence e-mail: mykhailo.s.shchetinin@lpnu.ua

Cite this article as: M. Shchetinin et al., *J. Nano- Electron. Phys.* 18 No 3, 03007 (2026) https://doi.org/10.21272/jnep.18(3).03007

ange-red emitter while achieving robust emissive performance. In this work, we proposed an OLED architecture and developed a device, featuring a quantum well structure, with the following layout. A previously synthesized D-A compound, incorporating a vinyltriphenylamine donor moiety and naphtalimide derivative acceptor-NI-3TPA was utilized as the orange-red emitter [8]. This material is highly sensitive to the surrounding environment and exhibits diverse photophysical properties across various media. Even its moderate ICT efficiency between the donor and acceptor moieties resulted in discrepancies in the photoluminescence maxima of the emitter across various solvents and the neat film (626 nm in THF, 560 nm in toluene and 584 nm in the film respectively). The observed solvatochromism is detrimental to devices operating in this and lower-energy spectral regions, as simultaneously achieving long-wavelength emission and high efficiency remains mutually exclusive. In other words, the efficiency of neat-film devices increases due to the blue shift of the spectra [9, 10].

2. EXPERIMENTAL SECTION

The precision control of functional nanoscale film thicknesses was performed in situ during the deposition process using a quartz crystal resonator. The change in the resonant frequency of the quartz resonator, monitored by a CH3-33 frequency counter, is highly sensitive to mass variations on the crystal plate where the film is deposited. The electrical and emissive characteristics of non-passivated organic structures were measured immediately after the fabrication of the organic heterostructures using a Hewlett-Packard 4145A parameter analyzer and a calibrated photodiode, while electroluminescence spectra were registered with an Ocean Optics USB2000 spectrometer according to the procedure described in [11].

3. DEVICE FABRICATION

The light-emitting structures were deposited onto glass substrates pre-coated with a 100 nm-thick indium tin oxide (ITO) layer. Before device deposition, the substrates were sequentially cleaned with isopropanol and distilled water, followed by ultrasonic treatment in acetone. The thin layers were sequentially deposited via thermal evaporation inside a vacuum chamber at a base pressure of 10-6 Torr. ITO serves as the transparent anode, while Al forms the cathode.

HAT-CN (1,4,5,8,9,11-hexaazatriphenylenehexacarbonitrile) this material is strongly electron-deficient, finds it's application as a hole-injection layer (HIL) [12]. Furthermore, for solution-processed OLEDs, HAT-CN is selectively soluble in 2-propanone but highly resistant to most other common casting solvents. This unique solubility prevents unwanted interfacial mixing and erosion of the underlayer during the deposition of top layers. The chemical structure of HAT-CN is shown in Figure 1. The energy of HOMO (highest occupied molecular orbital) and LUMO (lowest unoccupied molecular orbital) levels are 7.5 eV and 4.4 eV respectively.

TAPC (1,1-bis[4-[N,N-di(p-tolyl)amino]phenyl]cyclohexane) was employed as the hole transport layer (HTL) material. It also frequently functions as an electron-blocking layer or exciton-blocking layer (EBL) to confine excitons within the emissive layer. Along with HAT-CN it forms a p-blended hole-transporting layer (p-HTL) [13]. According to provided data by manufacturer, the HOMO and LUMO energy levels for this layer are as follows 5.5 eV and 2.0 eV. The triplet energy (T1) and singlet energy levels are reported as 2.87-2.9 eV and 3.26 eV respectively. TAPC exhibits high hole mobility and a shallow Homo level, which provides highly efficient hole injection and high current density into the device. Due to its high triplet energy (T1) and high-lying LUMO level, TAPC effectively confines excitons and blocks electrons from escaping the emissive layer, enhancing light coupling output. The chemical structure of TAPC is shown in Figure 1.

TCTA (4,4',4"-Tris(carbazol-9-yl)triphenylamine), served as a hole-transport and electron/exciton blocking buffer layer inserted between other transport layers (between TAPC and EML or mCBP in our case) to balance the process of hole injection [14]. Another feature of this material, when it utilized as a buffer or intermediate layer (e.g., placed between TAPC and EML or mCBP) its HOMO level effectively decreases the potential barrier for hole hopping, which improves charge balance and lowers driving voltages. The HOMO and LUMO energy levels equal 5.83 eV and 2.43eV respectively. The chemical structure of TCTA is shown in Figure 1.

TSPO1 (Diphenyl[4-(triphenylsilyl)phenyl]phosphine oxide), functions as an electron-transporting layer (ETL) and it is also utilized as a hole-blocking material due to its high HOMO energy level 6.79 eV. TSPO1 possesses a sufficiently high triplet energy (~ 3.2-3.3 eV) that enables it to effectively block excitons and suppress the triplet exciton quenching. The diphenylphosphine oxide substituent lowers its LUMO level, which facilitates efficient electron injection into the device [15]. The chemical structure of TSPO1 is shown in Figure 1.

TPBi (2,2',2"-(1,3,5-Benzinetriyl)-tris(1-phenyl-1-H-benzimidazole)), primarily functions as an electron-transporting layer (ETL) and hole-blocking layer (HBL) in the OLED architecture. TPBi features a LUMO level that reduces the barrier to electron injection from the cathode, while its inherent electron-transporting character increases overall electron mobility in the device. Due to its deep HOMO level material exhibits strong hole-blocking characteristics. This shifts the exciton recombination zone away from the cathode, effectively reducing cathode-induced electroluminescence quenching and improving overall device efficiency [16]. According to provided sources the HOMO and LUMO energy levels are 6.2/6.7 eV and 2.7eV. The triplet energy T1 is reported as 2.67 eV, and singlet energy S1 is reported as 3.70 eV. The chemical structure of TPBi is shown in Figure 1.

mCBP (3,3′-Di(9H-carbazol-9-yl)-1,1′-biphenyl) functions as a unipolar hole-type host material for emitters [17]. It acts as a thin intermediate layer (e.g. 5 nm thick on average) placed before the emissive layer to facilitate hole injection and prevent unwanted exciplex formation between adjacent layers. Because its HOMO level is 6.1 eV, it effectively reduces potential barriers and allows for "barrier-free" hole injection into emissive layer. The nanoscale film of this material facilitating the localization and balancing of holes and electrons within the potential well. The HOMO and LUMO energy levels are 6.0 eV and 2.4 eV, respectively. The chemical structure of mCBP is shown in Figure 1.

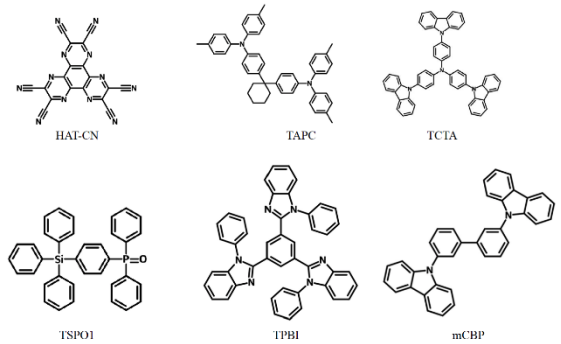

Fig. 1 – The general chemical structure of organic materials, which form the layer structure

Cs2CO3 (Cesium carbonate) was utilized as a electron injection layer (EIL) as this material is very efficient including in OLEDs based on small molecules [**Помилка! Джерело посилання не знайдено.**].

Moreover, considering that the confinement capacity of QW-based OLEDs is dependent on the number of periods and the width of the quantum wells [18], two OLEDs (Device B and Device C) featuring three quantum wells of varying widths (Fig. 2b) were fabricated via layer-by-layer thermal vacuum deposition.

Device A: HATCN (15 nm)/TAPC (40 nm)/TCTA (5 nm)/ NI-3TPA (25 nm)/TSPO1 (5 nm)/TPBi (45 nm)/Cs2CO3(0,5 nm)/Al (120 nm) fig. 2a).

Device B: HATCN (15 nm)/TAPC (40 nm)/TCTA (5 nm)/mCBP(7 nm)/ NI-3TPA(7 nm)/mCBP(7 nm)/ NI-3TPA(7 nm)/ mCBP(7 nm)/NI-3TPA (7 nm) /TSPO1 (5 nm)/TPBi (45 nm)/Cs2CO3(0,5 nm)/Al (120 nm)

Device C: HATCN (15 nm)/TAPC (40 nm)/TCTA (5 nm)/mCBP(3 nm)/ NI-3TPA(3 nm)/mCBP(3 nm)/ NI-3TPA(7 nm)/ mCBP(3 nm)/NI-3TPA (7 nm) /TSPO1 (5 nm)/TPBi (45 nm)/Cs2CO3(0,5 nm)/Al (120 nm).

The active area of each pixel in the fabricated structures is 2 mm × 2 mm.

4. RESULTS AND DESCUSSION

This study investigated the influence of the wide-bandgap mCBP layer thickness, as a constituent element of the mCBP/dey/mCBP potential well within the OLED architecture, on its electroluminescent characteristics. To this end, two OLEDs – Device B and Device C, were fabricated with mCBP layer thickness of 7nm and 3nm respectively (Fig. 2b). Device A, fabricated with a non-doped emissive layer (Fig. 2a), and the organic light-emitting diode D2, previously developed by the authors [8] based on host-guest technology (ITO/MoO3/TAPC/mCBP:NI-3TPA/TSPO1/TPBi/LiF/Al), were used as reference OLED structures to investigate the electroluminescent characteristics of QW-based OLEDs.

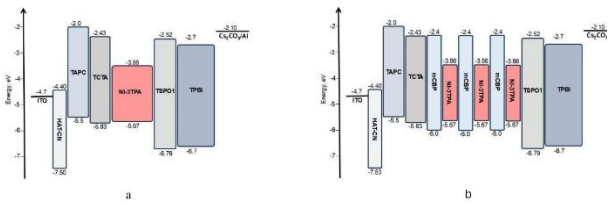

Fig. 2 – Energy diagram of the fabricated devices Device A (a) and Device B,C (b)

As observed from the current density-voltage and luminance-voltage characteristics (Fig. 3c-d, and Table 1), the turn-on voltage V_{on} of the triple-QW OLEDs increases from 5.6 V to 6.8 V as the mCBP layer thickness (barrier width) increases from 3 nm to 7 nm. The increase in the thickness of the wide-bandgap organic layer also negatively impacts the EQE, which consecutively drops from 5.1 % to 2.8 %, as well as the current efficiency CE of the devices. It is evident that under applied bias in Device C, the carrier tunnelling probability through 3 nm mCBP layer is significantly enhanced, which reduces exciton quenching caused by accumulated charges.

Consequently, a broader recombination zone and a uniform exciton distribution ultimately lead to enhanced device performance compared to Device B. As the potential well width increases, the electroluminescence undergoes a redshift from 566 nm to 578 nm (Fig. 3a).

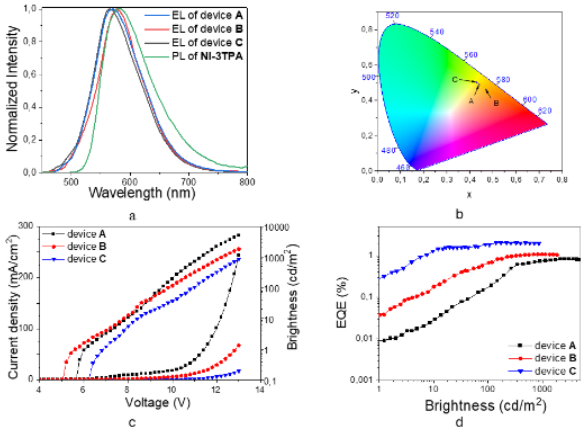

Fig. 3 – Normalized EL spectra recorded under the different voltages along with EML PL spectra (a),CIE1931 color coordinates (b) current density and luminance as a function of applied voltages (c) Fabricated devices EQE versus luminance (d)

Thus, the emission maximum approaches the values characteristic of Device A and Device D_2. The electroluminescence behavior of the QW-based OLED with a 13 nm potential well width is attributed to the enhanced quantum confinement effect [20], which improves the charge carrier localization within the potential well of the recombination zone. This results in a slight blue shift of the emission spectrum. It should be noted that the EQE of the reference orange non-doped Device A is only 0.83 % (Fig. 3d). A similarly low quantum efficiency is also characteristic if the previously developed Device D_2 [8], which exhibited an EQE of 0.5 % (Table 1).

In both devices, intermolecular interactions within the NI-3TPA film accelerate exciton quenching, leading to a rapid decline in efficiency. The electroluminescence spectrum of Device A was slightly blue-shifted relative to its photoluminescence spectrum (Fig. 3a). The minor discrepancies between the PL and EL spectra can be attributed to the different excitation mechanisms (optical versus electrical). It can be confidently asserted that electron-hole pair recombination occurs exclusively within the light-emitting layers of all investigated devices, as they exhibit consistent EL spectral profiles across wide range of applied voltages.

Table 1 – EL output and performance characteristics parameters of devices

Device	V_{on}, V	L, cd/m^2	CE, cd/A	EQE, %	PE, lm/W	λ_{EL}, nm	CIE1931, (x, y)
A neat film	5.1	5053	2.14	0.83	0.56	570	(0.44, 0.49)
B QW 1 (7 nm)	6.8	1845	2.79	1.07	0.75	578	(0.47, 0.46)
C QW 2 (3 nm)	5.6	858	5.11	2.03	1.40	566	(0.43, 0.50)
*D2	6.6	1470	0.4	0.5	1.2	586	(0.51, 0.47)

5. CONCLUSIONS

Based on the research results, it can be concluded that an orange-red emitting organic light-emitting diode was successfully developed. A distinctive feature of the device architecture is the incorporation of a triplet quantum well cascade, where nanoscale films of the wide-bandgap organic semiconductor mCBP encapsulate a narrow-bandgap ambipolar NI-3TPA emitter layer. Thus, in the developed QW-based OLED, both types of charge carriers are localized within the potential well layer due to the presence of the barrier layer, which enhances radiative recombination and suppresses the dissociation of fluorescent excitons. As the potential well mCBP/NI-3TPA/mCBP width increased from 13 to 21 nm, the EQE of the QW-based OLEDs decreased from 2.03 % to 1.07 %, while the emission maxima exhibited a redshift within the range of 566 nm to 578 nm. Compared to conventional doped devices, the NNT-OLEDs featuring a triple quantum well architecture based on the mCBP/NI-3TPA/mCBP stack demonstrated superior performance and advantages, including higher efficiency and stable reproducibility. Experimental results demonstrate that the development of QW-OLEDs utilizing suitable mCBP materials and moderate quantum well thicknesses is feasible and reproducible, enabling the achievement of high-efficiency OLEDs with tunable long-wavelength emission.

ACKNOWLEDGEMENTS

The authors acknowledge the financial support of this research by the National Research Foundation of Ukraine under the grant «Low-dimensional structures for enhancing the luminescence quantum yield in highly efficient phosphorescent light-emitting devices» (0124U003833).

The authors express their gratitude to the research group of Professor Juozas V. Grazulevičius of the Department of Polymer Chemistry and Technology of Kaunas University of Technology for kindly providing the emitter materials.

REFERENCES

1. J. Xue, Q. Liang, Y. Zhang, R. Zhang, L. Duan, J. Qiao, *Adv. Funct. Mater.* **27**, 1703283 (2017) https://doi.org/10.1002/adfm.201703283.
2. Q. Yu, Z. Deng, R. Chen, J. Zhang, R.T.K. Kwok, J.W.Y. Lam, J. Sun, B. Zhong Tang, *J. Am. Chem. Soc.* **147** No 12, 10530 (2025) https://doi.org/10.1021/jacs.4c18686.
3. Q. Zhang, H. Kuwabara, W.J. Potscavage Jr., Shuping Huang, Yasuhiro Hatae, Takumi Shibata, Chihaya Adachi, *J. Am. Chem. Soc.* **136** No 52, 18070 (2014). https://doi.org/10.1021/ja510144h.
4. X. Fu, A. Chen, Y. Yu, S. Hou, L. Liu, *Chem. Asian J.* **14**, 634 (2019) https://doi.org/10.1039/D0TA09496J.
5. S. Youn Lee, T. Yasuda, H. Nomura, C. Adachi, *Appl. Phys. Lett.* **101** No 9, 093306 (2012). https://doi.org/10.1063/1.4749285.
6. Yuichi Kitamoto, Taketo Namikawa, Dai Ikemizu, Yasuo Miyata, Takatsugu Suzuki, Hiroshi Kita, Tetsuo Sato‡a, Shuichi Oi, *J. Mater. Chem. C* **2**, 421 (2014). https://doi.org/10.1039/C5TC01380A.
7. L. Yingkui, *J. Lumin.* **131** No 9, 1821 (2011). https://doi.org/10.1016/j.jlumin.2011.04.048.
8. Naveen Masimukku, Malek Mahmoudi, Dmytro Volyniuk, Asta Dabuliene, Simas Macionis, Vitaly Matulis, Dmitry Lyakhov, Juozas V. Grazulevicius, *Spectrochimica Acta A: Mol. Biomol. Spectroscopy* **288**, 122185 (2023). https://doi.org/10.1016/j.saa.2022.122185
9. Y.-J. Yu, Y. Hu, S.-Y. Yang, W. Luo, Y. Yuan, C.-C. Peng, J.-F. Liu, A. Khan, Z.-Q. Jiang, L.-S. Liao, *Angew. Chem. Int. Ed.* **59**, 21578 (2020) https://doi.org/10.1002/anie.202006197.
10. Y. Sun, W. Sun, D. Zhang, J. Yin, M. Mao, L. Zhou, *J. Phys. Chem. C* **127** No 39, 19378 (2023) https://doi.org/10.1021/acs.jpcc.3c04174.
11. V.V. Cherpak, P.Y. Stakhira, D.Yu. Volynyuk, J. Simokaitiene, A. Tomkeviciene, J.V. Grazulevicius, A. Bucinskas, V.M. Yashchuk, A.V. Kukhta, I.N. Kukhta, V.V. Kosach, Z.Yu. Hotra, *Synthetic Metals* **161** No 13-14, 1343 (2011) https://doi.org/10.1016/j.synthmet.2011.04.035.
12. K. Yamaguchi, Y. Esaki, T. Matsushima, C. Adachi, *AIP Adv.* **10** No 5, 055304 (2020). https://doi.org/10.1063/5.0007310.
13. Y. Dai et al., *J. Mater. Chem. C* **3**, 6809 (2015) https://doi.org/10.1039/C4TC02875A.
14. Y-S. Tsai et al., *J. Luminescence* **153**, 312 (2014) http://dx.doi.org/10.1016/j.jlumin.2014.03.040.
15. D. Sun et al., *J. Mater. Chem. C* **3**, 9496 (2015). https://doi.org/10.1039/c5tc01638j.
16. T. D. Anthopoulos et al., *Appl. Phys. Lett.* **82**, 4824 (2003). https//doi.org/10.1063/1.1586999.
17. Y. Chen et al., *J. Mater. Chem. C* **5**, 8400 (2017) https://doi.org/10.1039/c7tc02406a.
18. J. Huang, Z. Xu, Y. Yang, *Adv. Funct. Mater.* **17** 1966 (2007) https://doi.org/10.1002/adfm.200700051.
19. Si-Hua Li et al., *J. Mater. Chem. C* **6**, 342 (2018) https://doi.org/10.1039/C8TC03287D.
20. W.K. Hew, K.J. Thomas, M. Pepper, I. Farrer, D. Anderson, G.A. Jones, D.A. Ritchie, *Phys Rev Lett.* **102** No 5, 056804 (2009) https://doi.org/10.1103/PhysRevLett.102.056804.

Органічний світловипромінювальний пристрій на основі квантової ями з настроюванням за кольором

М.С. Щетінін, С.А. Куцій, М.В. Гладун, І.Я. Яремчук, П.Й. Стахіра

Кафедра електронної інженерії, Національний університет «Львівська Політехніка», 79013 Львів, Україна

Розробка ефективних органічних світловипромінювальних діодів (OLED), зокрема на основі термоактивованої відкладеної флуоресценції (TADF), часто ускладнюється високим показником безвипромінювальної рекомбінації та гасінням екситонів у випадку плівки з чистого матеріалу, що є типовим процесом для складних архітектурних рішень на кшталт системи типу «гість-господар». У даному дослідженні запропоновано альтернативну архітектуру з послідовністю квантових ям, що дозволяє досягти контролю над кольором випромінювання та емісійними характеристиками. В якості емітера запропоновано використати сольватохромічний емітерний матеріал NI-3TPA. Використовуючи mCBP як широкозонний бар'єрний шар, було виготовлено OLED-структури з різною товщиною квантових ям (від 3 нм то 7 нм) та проведено систематичне оцінювання у порівнянні з нелегованим пристроєм, а також з еталонною структурою «гість-господар».

Результати демонструють що зміна товщини бар'єру mCBP безпосередньо впливає на електролюмінісцентні характеристики. Зокрема, зменшення товщини бар'єру до 3 нм підвищує ймовірність тунелювання носіїв заряду, що ефективно протидіє гасінню екситонів. Пристрій на основі квантових ям товщиною 3 нм продемонстрував нижчі значення напруги увімкнення (5,6 В) та досяг максимальної зовнішньої квантової ефективності (EQE) 2,03 %, що перевищує показники пристрою з бар'єром, товщиною 7 нм (1,07%) та пристрою на основі чистої плівки (0,83 %). Усі виготовлені зразки продемонстрували випромінювання в межах оранжево-червоної області координат CIE1931 системи колірності.

Запропонована архітектура дозволяє отримати точне налаштування спектра електролюмінісценції, демонструючи зсув у червону область випромінювання від 566 нм до 578 нм при збільшенні ширини потенціальної ями внаслідок ефекту квантового обмеження. В роботі пропонується підхід використання квантових ям, що не потребує складного технологічного процесу, який забезпечує відтворювальний підхід для локалізації носіїв заряду та екситонів у випромінювальному шарі, нівелюючи паразитні процеси та такі побічні ефекти як міжмолекулярне та екситонне гасіння.

Ключові слова: OLED, TADF, Квантова яма, Червоно-жовтий випромінювач, EQE.